PHYSICAL REVIEW A VOLUME 39, NUMBER 5 MARCH 1, 1989

Effects of initial-state population variations on the $2p \rightarrow 1s$ $K\alpha$ dielectronic satellite spectra of highly ionized iron ions in high-temperature astrophysical and laboratory plasmas

V. L. Jacobs
Condensed Matter and Radiation Sciences Division, Code 4603, Naval Research Laboratory, Washington, D.C. 20375-5000

G. A. Doschek and J. F. Seely
E.O. Hulburt Center for Space Research, Code 4170, Naval Research Laboratory, Washington, D.C. 20375-5000

R. D. Cowan
Los Alamos National Laboratory, Group T-4, Mail Stop MS-B212, P.O. Box 1663, Los Alamos, New Mexico 87545
(Received 15 August 1988)

Theoretical predictions are presented for the iron $K\alpha$ x-ray emission spectra from high-temperature plasmas, assuming steady-state optically thin excitation conditions. Account has been taken of all fine-structure components of the $2p \rightarrow 1s$ inner-shell-electron radiative transitions in the iron ions from Fe XVIII to Fe XXIV. The $K\alpha$ emission spectra are assumed to be produced by means of dielectronic recombination and inner-shell-electron collisional excitation processes that involve intermediate autoionizing states belonging to electronic configurations of the type $1s^1 2s^r 2p^s$. In addition to the electron-temperature variation, which is attributable to the temperature dependences of the radiationless electron capture and inner-shell-electron collisional excitation rate coefficients and to the temperature dependence of the charge-state distribution, the $K\alpha$ emission spectra exhibit an electron-density sensitivity. This electron-density sensitivity is a result of the density-dependent distribution of populations among the different fine-structure levels of the initial ions in the dielectronic recombination and inner-shell electron collisional excitation processes. In order to introduce a simplified treatment for the initial distribution of populations, whose precise determination would involve the detailed and self-consistent description of a multitude of elementary atomic autoionization, collision, and radiation processes, the electron-density range of interest has been subdivided into three, increasingly dense, regions. In the low-density region, which is expected to be appropriate for astrophysical plasmas such as solar flares and supernova remnants, it has been assumed that only the lowest-lying fine-structure levels of the ground-state electronic configurations of the initial ions are populated. Magnetically confined laboratory plasmas, such as tokamaks, are represented by the intermediate-density region, in which the initial ion populations have been assumed to be statistically distributed among all fine-structure levels of the ground-state electronic configurations. In the high-density region, which is expected to occur in laser-produced and vacuum-spark-produced plasmas, the populations of the initial ions have been assumed to be statistically distributed among all fine-structure levels of not only the ground-state electronic configurations but also the additional configurations which can be derived from the ground-state configurations by means of $2s \rightarrow 2p$ excitations. The inclusion of these additional excited configurations of the initial ions not only alters the intensities of the satellite lines that are predominant at low densities, but it also introduces additional satellite lines that occur at different wavelengths. Discussions are presented on the consequences of this electron-density sensitivity of the $K\alpha$ satellite emission for the spectroscopic determinations of electron temperatures, electron densities, and charge-state distributions in both astrophysical and laboratory plasmas.

I. INTRODUCTION

The dielectronic recombination and inner-shell electron collision excitation processes in highly ionized atomic ions have been known to be responsible for prominent features, known as dielectronic satellite lines, in the far-ultraviolet and x-ray emission spectra of high-temperature astrophysical and laboratory plasmas. These satellite lines have been identified on the long-wavelength sides of the associated resonance lines in low-density plasmas such as solar flares,[1,2] with electron densities $N_e \leq 10^{12}$ cm^{-3}, in intermediate-density plasmas such as encountered in the tokamak devices employed for magnetic confinement fusion research,[3,4] where $10^{13} \leq N_e \leq 10^{14}$ cm^{-3}, and in high-density laser-produced plasmas,[5,6] where $N_e \geq 10^{20}$ cm^{-3}. When the satellite lines are spectroscopically resolvable from the associated resonance line of the recombining ion, they can be utilized for

the determination of basic plasma properties, such as the electron temperature, the electron density, and the equilibrium and nonequilibrium charge-state distributions.[7,8] Unresolvable satellites usually represent radiative emissions that are indistinguishable from the resonance-line emission, and in certain cases they are known to provide substantial contributions to the observed resonance-line intensity. A noteworthy illustration of resolvable dielectronic satellite lines occurs in the case of the prominent $1s2p\ ^1P_1 \rightarrow 1s^2\ ^1S_0$ resonance line in the helium-like ion Fe XXV. This resonance line is often accompanied by conspicuous satellite features that are produced by radiatively stabilizing transitions of the general type $1s2pnl \rightarrow 1s^2nl$ in the lithiumlike ion Fe XXIV,[9-12] primarily with $n=2$ but also with some $n=3$ transitions corresponding to resolvable features. Since the unresolvable satellite lines, which mainly correspond to $n \geq 3$, occur in a Rydberg series with decreasing wavelength displacements from the position of the resonance line, the enhancement in the apparent intensity of the resonance line is accompanied by an asymmetric broadening. Simplified calculations,[13] utilizing LS- and fine-structure-averaged atomic transition rates, are expected to be adequate for the evaluation of the total dielectronic recombination rate resulting from the multitude of satellite transitions. This total rate has been established by Burgess[14] to be the dominant recombination rate for multiply charged nonhydrogenic ions in low-density, high-temperature plasmas. However, a detailed and self-consistent treatment of the elementary autoionization, collision, and radiation processes, utilizing the transition rates connecting individual fine-structure states, is expected to be essential for the accurate analysis and interpretation of high-resolution dielectronic satellite spectra. An additional motivation for the increasing emphasis toward more refined calculations for dielectronic satellite radiation processes is provided by the recent demonstration[15,16] that the total dielectronic recombination rate for high-Z atomic ions, with $Z \geq 30$, is determined, in the important temperature region, predominantly by the contributions from the energetically lowest-lying autoionizing levels. These autoionizing levels are responsible for the resolvable dielectronic satellite lines.

In this investigation theoretical results are presented for the $K\alpha$ satellite emission spectra produced by the $2p \rightarrow 1s$ inner-shell electron radiative transitions in the iron ions from Fe XVIII to Fe XXIV. These radiative transitions give rise to prominent satellite lines in the x-ray region from 1.85 to 1.93 Å. The $K\alpha$ satellite spectra of iron have been observed with high resolution from solar flares,[1,2,17,18] with $N_e \leq 10^{12}$ cm^{-3}, from the Princeton large torus tokamak device,[3,4,19,20] with $10^{13} \leq N_e \leq 10^{14}$ cm^{-3}; and from vacuum sparks[21] and laser-produced plasmas,[22] with $N_e \geq 10^{20}$ cm^{-3}. The $K\alpha$ satellite emission spectra of iron have been the subject of previous theoretical investigations for tokamak-plasma conditions, the first of which was reported by Merts, Cowan, and Magee.[23] These investigators allowed for dielectronic recombination and inner-shell electron collisional excitation processes from the ground-state electronic configurations of the initial ions. In particular, they assumed that the initial ion populations are statistically distributed among the various fine-structure levels. The dielectronic recombination and the inner-shell electron collisional excitation mechanisms involve intermediate autoionization-resonance configurations of the type $1s^12s^r2p^s$, in which the K-shell vacancy initially formed by either radiationless electron capture or inner-shell electron collisional excitation may be filled by either a $2p \rightarrow 1s$ radiatively stabilizing transition or an autoionization process. The various autoionization and spontaneous radiative transition rates, which are required for the prediction of the satellite-line intensities, were evaluated by utilizing the relativistic multiconfiguration atomic structure code of Cowan.[24] Merts, Cowan, and Magee[23] also included the additional contributions to the satellite emission spectra which are produced by radiative transitions from autoionizing configurations of the general type $1s^12s^r2p^snl$, with $n \geq 3$, and they took into account the additional contributions that correspond to inner-shell electron collisional ionization processes. They concluded, however, that these additional contributions did not result in a substantial modification of the predicted satellite emission spectra for the iron ions from Fe XVIII to Fe XXIV. They also pointed out that, in most cases, the dielectronic recombination process provides the dominant contribution to the satellite-line intensities. However, there are particular satellite transitions for which the inner-shell electron collisional excitation process is found to be important.

In a subsequent application of the investigation by Merts, Cowan, and Magee[23] to solar-flare plasma conditions, Doschek, Feldman, and Cowan[25] imposed the appropriate low-density excitation condition that both the dielectronic recombination and the inner-shell electron collisional excitation processes can occur only from the energetically lowest-lying fine-structure levels of the ground-state electronic configurations of the initial ions. In further extensions of this investigations, by Phillips, Lemen, Cowan, Doschek, and Leibacher[26] and by Lemen, Phillips, Doschek, and Cowan,[27] $K\alpha$ satellite emission spectra have been predicted for both solar-flare and tokamak-plasma conditions by means of a detailed calculation (utilizing the individual bound-bound atomic collisional and radiative transition rates) of the electron-density-dependent population distributions of the initial ions among the entire sets of fine-structure levels belonging to the ground-state electronic configurations. The $K\alpha$ satellite emission spectra predicted in these extensions[26,27] exhibit a conspicuous electron-density sensitivity in the range $10^{13} \leq N_e \leq 10^{15}$ cm^{-3}, which is of particular interest in magnetic-fusion research.

In order to develop a more extensive model, which would enable the prediction of the $K\alpha$ satellite emission spectra to be made over a wider range of electron densities, it will be necessary to remove the restriction of taking into account only processes involving the ground-state electronic configurations of the initial iron ions. In particular, it would be desirable to extend the calculations for the $K\alpha$ satellite emission spectra to the electron-density region $10^{19} \leq N_e \leq 10^{24}$ cm^{-3}. In this high-electron-density region, the $2s \rightarrow 2p$ collisional exci-

tations of the ground-state configurations are more efficient than the corresponding $2p \rightarrow 2s$ spontaneous radiative transitions. However, the corresponding collisional excitation and de-excitation processes among the autoionizing levels are not yet competitive with the $2p \rightarrow 1s$ autoionization and radiative stabilization processes. In this high-density region, which occurs in laser-produced and vacuum-spark-produced plasmas, both the dielectronic recombination and the inner-shell electron collisional excitation processes can occur not only from iron ions initially in their ground-state electronic configurations but also from iron ions initially in the electronic configurations which can be derived from the ground-state configuration by means of $2s \rightarrow 2p$ excitations. Examples of such excited electronic configurations have been included in a previous investigation of the $K\alpha$ satellite emission spectra of iron for solar-flare conditions by Mewe, Schrijver, and Sylwester[28] and by Mewe and Schrijver,[29] but these investigators apparently did not take into account the correct electron-density dependences of the population distributions associated with the initial ions in these excited electronic configurations. It has been pointed out by Doschek, Feldman, and Cowan[25] that the processes involving the initial ions in these excited electronic configurations cannot appreciably contribute to the satellite emission spectra except at the orders-of-magnitude higher densities that are characteristic of laser-produced and vacuum-spark-produced plasmas.

In the present investigation we have systematically taken into account all fine-structure components of the satellite transitions that are produced by both the dielectronic recombination and the inner-shell electron collisional excitation processes in the iron ions from Fe XVIII to Fe XXIV. In order to obtain predictions appropriate for each of the three particular electron-density regions of interest, we have performed three separate calculations. In the low-density region appropriate for solar-flare plasma conditions, we have assumed that the initial ion populations are confined to the lowest-lying fine-structure levels of the ground-state electronic configurations. In the intermediate-density region appropriate to tokamak plasmas, we have assumed that the initial ion populations are statistically distributed among all fine-structure levels of the ground-state electronic configurations. Finally, in the high-density region corresponding to laser-produced and vacuum-spark-produced plasmas, we have assumed that the initial ion populations are statistically distributed among all fine-structure levels of both the ground-state electronic configurations and the additional electronic configurations that can be formed by means of the possible $2s \rightarrow 2p$ excitations.

The theoretical treatment of the satellite emission spectra which is employed in the present investigation has been described for heliumlike and lithiumlike ions by Jacobs, Rogerson, Chen, and Cowan.[30] This theoretical treatment may be regarded as a systematic extension of an earlier investigation, which has been reported by Jacobs and Blaha,[31] to incorporate the fine-structure splittings of the LS components of the satellite lines and the effects of the quantum-mechanical interference between the autoionization and spontaneous radiative decay modes.[32–34] In subsequent theoretical investigations[35,36] expressions have been derived for the combined electron-ion photorecombination cross section which incorporate the additional interference between the transition amplitudes corresponding to radiative and dielectronic recombination, but numerical results have not yet been obtained from the unified theory of radiative and dielectronic recombination. The earlier investigation by Jacobs and Blaha[31] was concerned primarily with the effects of $2s \rightarrow 2p$ angular-momentum-changing collisional transitions among the autoionizing-resonance levels, which become important only in the very-high-electron-density region $N_e \geq 10^{24}$ cm^{-3}. Since neither the angular-momentum-changing collisional transitions among the autoionizing levels nor the quantum-mechanical interference effects will be investigated in the present calculations for the $K\alpha$ satellite emission spectra of iron, our theoretical treatment is a natural extension of the theory described by Cowan[24] and employed by Merts, Cowan, and Magee[23] and by the subsequent investigators.[25–27]

For precise theoretical predictions of the dielectronic satellite emission spectra, it is necessary to incorporate not only a systematic and detailed treatment of the individual fine-structure components of the satellite-line intensities but also an accurate determination of the satellite transition-wavelength positions together with a realistic representation of the satellite-line profile functions. It has been demonstrated by Seely, Feldman, and Safronova[37] that the theoretically predicted wavelengths for the $2p \rightarrow 1s$ inner-shell electron transitions in the iron ions from Fe XVIII to Fe XXIV, which have been obtained from the multiconfiguration relativistic atomic structure code of Cowan,[24] must be systematically corrected in order to obtain precise agreement with the measured wavelengths, which have been derived from high-resolution x-ray emission spectra. The required transition-wavelength corrections, which are between 0.002 and 0.003 Å for these iron ions, are partially due to the incomplete representation of the nonrelativistic and relativistic contributions to the many-electron energy eigenvalues but are mainly attributable to quantum electrodynamical energy corrections,[38,39] which in lowest-order perturbation theory include the electron self-energies and the vacuum-polarization energies.

The Doppler broadening produced by the thermal or turbulent motion of the radiating ions is expected to be the dominant spectral-line-broadening mechanism in a low-density high-temperature plasma. The satellite lines are also broadened by the action of the electric and magnetic plasma microfield fluctuations[40] and by the same elementary atomic autoionization, collision, and radiation processes which enter into the determination of the population densities of the upper and lower levels in the radiatively stabilizing transitions. In the isolated-line approximation,[41] the emission spectra produced by a particular array of radiatively stabilizing transitions can be represented in terms of a superposition of Voigt line-profile functions, which are convolutions of a Gaussian profile function representing the Doppler broadening and

a Lorentzian profile function describing the broadening that is due to the elementary atomic autoionization, collision, and radiation processes. The complete determination of the spectal-line broadening profile functions, which would be valid over an extensive electron-density range extending above $N_e = 10^{24}$ cm^{-3}, must take into account the additional phenomenon of Stark broadening. Such a determination would represent a substantial effort for the multitude of satellite transitions that have been taken into account in this investigation. Rather than attempt such a full treatment of the spectral-line-broadening problem, we have employed only the Doppler line-profile functions in the evaluation of the theoretical satellite emission spectra. We have, however, obtained an assessment of the adequacy of this Gaussian-profile approximation in the various density regions of interest by means of a systematic evaluation of the Voigt line-profile parameters.

The remainder of this paper has been organized in the following manner. In Sec. II we present a review of the theory of the dielectronic satellite emission spectra, taking into account the spectral-line formation processes of dielectronic recombination and inner-shell-electron collisional excitation. We also include a detailed discussion of the simplified treatments of the initial-ion level-population distribution which have been adopted for the three separate electron-density regions of interest. A detailed description of the calculations is presented in Sec. III, together with the predicted $K\alpha$ satellite emission spectra that have been obtained for the iron ions from Fe XVIII to Fe XXIV. For each of the three separate electron-density regions, we present two sets of calculations, which correspond to the electron temperatures $T_e = 1.0\times10^7$ and 2.0×10^7 K. We also present a discussion of the qualitative differences among the theoretical results that have been obtained using the three different initial-ion level-population distributions, and we attempt to make a comparison with available observed spectra from plasmas corresponding to the three different electron-density regions. Our conclusions are presented in Sec. IV, together with a further discussion of the additional refinements that should be incorporated into future extensions of this investigation.

II. THEORY OF DIELECTRONIC SATELLITE SPECTRA

The theory of dielectronic satellite spectra which is described in this section is based on the formalism that has been presented in a recent investigation by Jacobs, Rogerson, Chen, and Cowan.[30] However, an alternative designation for the atomic states has now been adopted in order to conform with the notation employed in the theory of dielectronic recombination and inner-shell-electron collisional excitation which is presented in the recent book by Cowan.[24] Our objective has been to develop simplified treatments for the three different electron-density regions of interest.

We denote by j an autoionizing state of the N-electron ion X^{z+} with residual charge z, which is related to the nuclear charge Z by $z = Z - N$. The satellite spectra of interest in this investigation are produced by the radiatively stabilizing transitions

$$X^{z+}(j) \rightarrow X^{z+}(k) + h\nu \ , \tag{1}$$

in which the final state k lies below the ionization threshold. In the isolated-line approximation,[41] the emission spectra produced by the entire array of radiatively stabilizing transitions $j \rightarrow k$ can be represented in the form

$$\epsilon(h\nu) = (h\nu/4\pi) \sum_j \sum_k N(j) A_r(j \rightarrow k) L(j \rightarrow k, h\nu) \ , \tag{2}$$

which gives the power radiated per unit volume per unit solid angle and photon-energy intervals. The population densities of the ions in the autoionizing levels j are denoted by $N(j)$, the rates at which photons with energy $h\nu$ are spontaneously emitted are represented by $A_r(j \rightarrow k)$, and the photon-energy-normalized line-shape functions are designated by $L(j \rightarrow k, h\nu)$. Although the population densities $N(j)$ employed in the present investigation have been obtained from a steady-state excitation model, Eq. (2) can be applied to nonequilibrium excitation conditions, for which the population densities must be obtained from the time-dependent rate equations. Since the population densities $N(j)$ will depend on the hydrodynamic variables that characterize the physical conditions within the plasma, such as the electron and ion temperatures and the electron and ion densities, the satellite spectra represented by the emission coefficient of Eq. (2) will be functions of these temperatures and densities. The summations over j and k must include all transitions that can contribute within the photon-energy range of interest. In this investigation, we have taken into account all fine-structure components of the $2p \rightarrow 1s$ transitions which are produced by the radiative stabilization processes from autoionizing states belonging to the electronic configurations $1s^1 2s^r 2p^s$ (with $0 \le r \le 2$ and $0 \le s \le 6$) in the iron ions from Fe XVIII to Fe XXIV.

The review of the theory of dielectronic satellite spectra which is presented below has been subdivided according to the individual line-formation mechanisms by means of which the autoionizing levels j can be populated.

A. Dielectronic recombination

The autonizing state j, which will be specified in terms of the total electronic angular momentum J, can be populated by means of the radiationless electron capture process

$$X^{(z+1)+}(m) + e^-(\varepsilon_{jm}) \rightarrow X^{z+}(j) \ , \tag{3}$$

where m denotes the initial fine-structure state of the recombining ion $X^{(z+1)+}$ and ε_{jm} is the energy of the captured electron. If the radiationless electron capture rate coefficient is denoted by $C_{\rm cap}(m\varepsilon_{jm} \rightarrow j)$, the corresponding contribution to the steady-state population density of the autoionizing level j can be expressed in the form[31]

$$[N(j)]_{\text{cap}}=\sum_{j'}\sum_{m}Q^{-1}(j,j')C_{\text{cap}}(m\varepsilon_{j'm}\rightarrow j')N(m)N_e\ , \tag{4}$$

where Q^{-1} denotes the matrix of the autoionization, collisional, and radiative transition rates which have been taken into account in the determination of the steady-state population densities of the autoionizing levels j. The number density of recombining ions initially in the fine-structure level m is denoted by $N(m)$.

In the corona-equilibrium-model approximation,[13,14] which is valid at sufficiently low plasma densities, it is assumed that all excited levels of the atomic system are depopulated only by means of autoionization or by means of spontaneous radiative emission processes. In this approximation, the only nonvanishing elements of the transition rate matrix Q are the diagonal elements given by[30]

$$Q(j,j)=\sum_{m'}A_a(j\rightarrow m'\varepsilon_{jm'})+\sum_{k'}A_r(j\rightarrow k')\ , \tag{5}$$

which is the sum of the rates $A_a(j\rightarrow m'\varepsilon_{jm'})$ for autoionization into all energetically accessible fine-structure states m' of the recombining ion and the sum of the rates $A_r(j\rightarrow k')$ for spontaneous radiative transitions to all lower fine-structure states k' of the recombined atomic system. If nonstabilizing radiative transitions to lower-lying autoionizing states are permissible, then the nonstabilizing radiative transitions cannot be consistently taken into account in Eq. (5) without also allowing for these additional spontaneous radiative processes in the nondiagonal elements of the transition rate matrix Q.

For a Maxwellian distribution of incident electron energies, the radiationless electron-capture rate coefficient $C_{\text{cap}}(m\varepsilon_{jm}\rightarrow j)$ can be expressed, in terms of the autoionization rate $A_a(j\rightarrow m\varepsilon_{jm})$, by means of the detailed balance relationship[7]

$$C_{\text{cap}}(m\varepsilon_{jm}\rightarrow j)=2^3a_0^3\pi^{3/2}(g_j/2g_m)(E_H/k_BT_e)^{3/2}\times\exp[-(\varepsilon_{jm}/k_BT_e)]A_a(j\rightarrow m\varepsilon_{jm})\ , \tag{6}$$

where g_j and g_m represent, respectively, the statistical weights of the autoionizing level j and of the recombining-ion fine-structure level m, T_e is the electron temperature, k_B is the Boltzmann constant, a_0 is the Bohr radius, and E_H is the ionization energy of atomic hydrogen.

It has been suggested[42] that an analysis of the line spectra produced by the satellite transitions in the lithiumlike iron ion Fe XXIV, together with the resonance transition in the heliumlike iron ion Fe XXV, can provide a determination of the population of nonthermal electrons. Nonthermal electrons may be produced by the action of strong electric, magnetic, or laser-radiation fields, particularly in low-density plasmas where collisional relaxation processes among electrons tend to be less efficient than the collisionless mechanisms. This technique has been recently implemented[43] to deduce from spectral observations evidence for the presence of a nonthermal component of the electron-energy distribution. For non-Maxwellian electron-energy distributions, the appropriate generalization of Eq. (6) must be employed.

It is convenient to introduce the photon emission rate coefficient (which is measured in $\text{cm}^3\,\text{sec}^{-1}$) for dielectronic recombination as follows:[30]

$$\alpha_{\text{DR}}(m\varepsilon_{jm}\rightarrow j\rightarrow k)=\sum_{j'}A_r(j\rightarrow k)Q^{-1}(j,j')\times C_{\text{cap}}(m\varepsilon_{j'm}\rightarrow j')\ . \tag{7}$$

If we take into account only the diagonal Q-matrix elements with $j=j'$, the factor $A_r(j\rightarrow k)Q^{-1}(j,j)$ becomes equivalent to the familiar branching ratio for the radiatively stabilizing transition $j\rightarrow k$, which is conventionally denoted by $B_r(j\rightarrow k)$. If self-absorption of the satellite radiation by the plasma is ignored, the dielectronic recombination contribution to the total angle- and frequency-integrated emitted-photon intensity (measured in $\text{cm}^{-3}\,\text{sec}^{-1}$) can be expressed as[30]

$$I_{\text{DR}}(j\rightarrow k)=\sum_{m}\alpha_{\text{DR}}(m\varepsilon_{jm}\rightarrow j\rightarrow k)N(m)N_e\ . \tag{8}$$

At very low electron densities ($N_e\leq 10^{10}\ \text{cm}^{-3}$), only the lowest-lying fine-structure level m_0 of the ground-state electronic configuration of the recombining ions will attain an appreciable population density. Consequently, it will be necessary to retain only the m_0 contribution to the summation over m in Eq. (8). This assumption is expected to be valid for the highly ionized iron ions in the low-density regions of the solar corona.

In the intermediate-density plasmas that are of interest in magnetic confinement fusion research ($10^{13}\leq N_e\leq 10^{14}\ \text{cm}^{-3}$), the collisional excitation rates may become sufficiently high to establish a statistical distribution of the population density among the metastable fine-structure levels of the ground-state electronic configuration, which can undergo spontaneous radiative decay only by means of relatively weak optically forbidden (magnetic-dipole, electric-quadrupole, etc.) transitions. Consequently, the distribution of population among the various fine-structure levels m of the ground-state electronic configuration can be approximated by means of the statistical relationship

$$\frac{N(m)}{N_{z+1}}=\frac{g_m}{\sum_m g_m}\ , \tag{9}$$

where the summation over m is to be taken over all fine-structure levels of the ground-state electronic configuration and N_{z+1} represents the total number density of the initial ions $X^{(z+1)+}$, which are assumed to be predominantly in the fine-structure levels of the ground-state electronic configuration. It is now customary to introduce for the radiatively stabilizing transition $j\rightarrow k$ the average dielectronic recombination rate coefficient $\alpha_{\text{DR}}(j\rightarrow k)$, which is defined so that the dielectronic recombination contribution to the photon intensity, radiated per unit volume in the satellite transition $j\rightarrow k$, can be expressed in the form

$$I_{\text{DR}}(j\rightarrow k)=\alpha_{\text{DR}}(j\rightarrow k)N_{z+1}N_e\ . \tag{10}$$

The appropriate average dielectronic recombination rate coefficieint can be determined from an evaluation of the expression

$$\alpha_{\mathrm{DR}}(j\rightarrow k)=4\pi^{3/2}a_0^3(E_H/k_BT_e)^{3/2}\exp[-(\varepsilon_{j0}/k_BT_e)] \times\left[g_j\Big/\sum_m g_m\right]A_r(j\rightarrow k)Q^{-1}(j,j) \times\sum_m A_a(j\rightarrow m\varepsilon_{jm}) , \quad (11)$$

where the summations over m are to be taken over all fine-structure levels of the ground-state electronic configuration and ε_{j0} represents an appropriate average value of the electron energy.

In the present investigation we also consider the high-density region $10^{20}\leq N_e\leq 10^{24}$ cm^{-3}, which is characteristic of laser-produced and vacuum-spark-produced plasmas. In this density region, the collisional excitation rates are expected to be sufficiently high to establish a statistical distribution of the initial-ion populations not only among the fine-structure levels of the ground-state electronic configuration but also among the fine-structure levels corresponding to all additional electronic configurations that can be derived from the ground-state electronic configuration by means of $2s\rightarrow 2p$ excitations. Consequently, the summations over m in Eqs. (9) and (11) are now to be extended to include the additional fine-structure levels of the excited electronic configurations.

It should be emphasized that, for an accurate determination of the dielectronic satellite spectra, it will be necessary in a future extension of this investigation to obtain the actual initial-ion fine-structure-level populations from a detailed and self-consistent collisional-radiative-equilibrium model calculation, in which systematic account would be taken of all relevant autoionization, collisional, and radiative transition rates.

B. Inner-shell-electron collisional excitation

Alternatively, the autoionizing state j can be populated as a result of the inner-shell-electron collisional excitation process

$$X^{z+}(k'')+e^-(\varepsilon_{k''})\rightarrow X^{z+}(j)+e^-(\varepsilon_j) , \quad (12)$$

where k'' is a bound fine-structure state of the ion X^{z+}. If the inner-shell-electron collisional-excitation rate coefficient is denoted by $C_e(k''\rightarrow j)$, the contribution from this electron-impact excitation process to the steady-state population density of the autoionizing level j can be written in the form[31]

$$[N(j)]_{\mathrm{exc}}=\sum_{j'}\sum_{k''}Q^{-1}(j,j')C_e(k''\rightarrow j')N(k'')N_e , \quad (13)$$

where, in the corona-equilibrium-model approximation, the transition rate matrix Q has only diagonal matrix elements, which are given by Eq. (5). The population density of the initial ions in the bound fine-structure state k'' is denoted by $N(k'')$.

For a Maxwellian distribution of incident electron energies, the inner-shell-electron collisional-excitation rate coefficient $C_e(k''\rightarrow j)$ can be expressed, in terms of the spontaneous radiative transition rate $A_r(j\rightarrow k'')$, by employing the Bethe approximation[44]

$$C_e(k''\rightarrow j)=(32/3^{1/2})\pi^{3/2}(g_j/g_{k''})(a_0/\alpha)^3[E_H/\Delta E(k''\rightarrow j)]^2(E_H/k_BT_e)^{3/2}[k_BT_e/\Delta E(k''\rightarrow j)] \times(3^{1/2}/2\pi)\{(\ln 4)\exp[-\Delta E(k''\rightarrow j)/k_BT_e]+E_1[\Delta E(k''\rightarrow j)/k_bT_e]\}A_r(j\rightarrow k'') , \quad (14)$$

which is applicable only to electric-dipole transitions. Since single-electron electric-dipole transitions are expected to be associated with the most rapid collisional excitation processes, the use of the Bethe approximation for the collisional-excitation rate coefficients should be adequate for the present investigation. For selected $1s\rightarrow 2p$ transitions in heliumlike and lithiumlike argon ions, the electron collisional-excitation rate coefficients which have been obtained using the Bethe approximation have been compared[30] with the corresponding results of more elaborate distorted-wave calculations.[45] The agreement between the results obtained by means of the two different procedures has been found to be much closer than had been anticipated. Further improvement in the agreement between the two results can be obtained[31] by the introduction of a reduction factor of 0.5 in the Bethe cross section, which yields good agreement with the threshold values of the distorted-wave cross sections. This procedure has been adopted in the present calculations.

In a form analogous to Eq. (7), we may introduce the photon emission rate coefficient for collisional excitation of the radiative transition $j\rightarrow k$ as[30]

$$C_{\mathrm{CE}}(k''\rightarrow j\rightarrow k)=\sum_{j'}A_r(j\rightarrow k)Q^{-1}(j,j')C_e(k''\rightarrow j') . \quad (15)$$

The collisional-excitation contribution to the total rate of photon emission per unit volume in the satellite transition $j\rightarrow k$ can then be expressed in the form[30]

$$I_{\mathrm{CE}}(j\rightarrow k)=\sum_{k''}C_{\mathrm{CE}}(k''\rightarrow j\rightarrow k)N(k'')N_e . \quad (16)$$

As discussed in Sec. II A in connection with the population densities of the fine-structure levels m of the recombining ion, we will subdivide the electron-density range of interest into three, increasingly dense regions in order to introduce a simplified treatment for the distribution of population density among the bound fine-structure levels k'' of the combined ion. In the very-low-density region, it will be necessary to retain only the k_0'' contribution in the summation over k'' in Eq. (16). In

the intermediate- and high-density regions, we will introduce the statistical distributions

$$\frac{N(k'')}{N_z}=\frac{g_{k''}}{\sum_{k''} g_{k''}} , \tag{17}$$

where the summation over k'' is to be taken over all fine-structure levels of either only the ground-state electronic configuration or the ground-state electronic configuration together with the additional electronic configurations that can be formed by means of $2s \rightarrow 2p$ $\Delta n=0$ excitations. In either case, N_z represents the total number density of the combined ions X^{z+}.

For the statistical distributions of the population densities $N(k'')$, it is convenient to introduce the average inner-shell-electron collisional-excitation rate coefficient $C_{\mathrm{CE}}(j \rightarrow k)$, which is defined so that the collisional-excitation contribution to the photon intensity radiated in the satellite transition $j \rightarrow k$ can be expressed in the form

$$I_{\mathrm{CE}}(j \rightarrow k)=C_{\mathrm{CE}}(j \rightarrow k) N_z N_e . \tag{18}$$

The appropriate average collisional-excitation rate coefficient can be evaluated by means of the expression

$$\begin{aligned} C_{\mathrm{CE}}(j \rightarrow k)=&(32/3^{1/2})\pi^{3/2}(a_0/\alpha)^3[E_H/\Delta E(0 \rightarrow j)]^2(E_H/k_B T_e)^{3/2}[k_B T_e/\Delta E(0 \rightarrow j)] \\ &\times(3^{1/2}/2\pi)\{(\ln 4)\exp[-\Delta E(0 \rightarrow j)/k_B T_e]+E_1[\Delta E(0 \rightarrow j)/k_B T_e]\} \\ &\times\left[g_j/\sum_{k''} g_{k''}\right] A_r(j \rightarrow k) Q^{-1}(j,j) \sum_{k''} A_r(j \rightarrow k'') , \end{aligned} \tag{19}$$

where the summations over k'' are to be taken over all bound fine-structure levels of the electronic configurations and $\Delta E(0 \rightarrow j)$ represents an appropriate average value of the excitation energy.

C. Additional excitation processes

Inner-shell-electron collisional ionization may represent the most important excitation mechanism for the autoionizing states which has not been taken into account in the present investigation. A comprehensive investigation of radiative and Auger emission following inner-shell-electron ionization of iron ions has been presented,[46] in which systematic account has been taken of all elementary Auger processes and spontaneous radiative transitions that can occur during the inner-shell vacancy cascade decay process. However, in order to allow for the multitude of permissible transitions, it was necessary to employ transition rates which had been averaged over both the LS structure and fine structure of the atomic levels. An important characteristic of the complex vacancy cascade decay processes, which is properly treated in this comprehensive description,[46] is that autoionizing levels corresponding to multiple-vacancy states can be populated as a result of Auger processes following the creation of deep single-electron inner-shell vacancy distributions. In the presence of intense radiation fields near the satellite transition wavelengths, which can occur in optically thick regions of the plasma,[47] it would be necessary to take into account photoexcitation, photoionization, and perhaps even photon-induced electron-capture processes.

III. DESCRIPTION OF THE CALCULATIONS AND DISCUSSION OF THE THEORETICALLY PREDICTED $K\alpha$ SATELLITE EMISSION SPECTRA

The relativistic multiconfiguration atomic-structure program developed by Cowan[24] has been employed to obtain the photon wavelengths, together with the autoionization and spontaneous radiative decay rates, for all $2p \rightarrow 1s$ inner-shell electric-dipole radiative transitions which involve autoionizing states belonging to electronic configurations of the type $1s^1 2s^r 2p^s$, with $0 \leq r \leq 2$ and $0 \leq s \leq 6$, in the iron ions from Fe XVIII to Fe XXIV. The electric-dipole radiative transitions which have been taken into account for each ion are specified, according to the initial and final electronic configurations, in Table I, which also indicates the total number of fine-structure components in each case. This table provides a concise presentation of the organization of our calculations. In particular, we have listed for each radiative transition the ground-state electronic configuration followed by the excited electronic configurations of the initial ions, from which the autoionizing states can be formed as intermediate states in the dielectronic recombination processes. While the first entry for each ion corresponds to spontaneous radiative transitions to the ground-state electronic configuration of the recombined ion, additional entires refer to spontaneous radiative transitions terminating on bound excited electronic configurations. In addition to the dielectronic recombination processes, the various spontaneous radiative transitions can be produced by means of inner-shell-electron collision-excitation processes from ions initially in either the ground-state or the bound excited electronic configurations. In our calculations appropriate to the high-density region, all ground-state and bound excited electronic configurations in Table I have been taken into account. A very large number of fine-structure components was required for the calculations in the high-density region, especially in the case of Fe XXI and Fe XXII. The number of required fine-structure components was reduced substantially in the intermediate-density-region calculations, for which we have assumed that both the dielectronic recombination and the inner-shell-electron collisional-excitation processes can occur only from ions initially in the ground-state electronic configurations. Finally, only a very limited number of fine-structure components was required for the calculations in the low-density region, for which we have

assumed that all ions are initially confined to their ground-state fine-structure levels.

It should be emphasized that spontaneous radiative emission processes corresponding to two-electron transitions have not been included in our calculations. Their exclusion is the result of the use in our atomic structure calculations of a limited basis set of atomic states, consisting of only a single autoionizing configuration and a single bound-state configuration for each separate spontaneous radiative transition in Table I. The two-electron spontaneous radiative transitions, which would result from the inclusion of configuration mixing, are not expected to provide significant contributions to the iron $K\alpha$ satellite intensities. The only two allowed two-electron spontaneous radiative transitions that can occur in the lithiumlike ion Fe XXIV have been included in Fig. 1, which schematically illustrates the complete array of $n=2$ satellite transitions for this ion. In this figure the various fine-structure components of the Fe XXIV satellite transitions have been designated according to the alpha-

TABLE I. $2p \rightarrow 1s$ inner-shell-electron electric-dipole spontaneous radiative transitions which have been taken into account in the theoretical predictions of the iron $K\alpha$ satellite emission spectra. These radiative transitions can be produced both by the corresponding inner-shell-electron collisional-excitation processes and by the dielectronic recombination processes, which in some cases can occur from bound excited electronic configurations of the recombining ion.

Fe ion	Initial and final configurations	Recombining ion configurations	Number of fine-structure components
Fe XVIII	$1s2s^22p^6 \rightarrow 1s^22s^22p^5$	$1s^22s^22p^4$	2
		$1s^22s^12p^5$	2
		$1s^22s^02p^6$	2
Fe XIX	$1s2s^22p^5 \rightarrow 1s^22s^22p^4$	$1s^22s^22p^3$	14
		$1s^22s^12p^4$	14
		$1s^22s^02p^5$	14
Fe XIX	$1s2s^12p^6 \rightarrow 1s^22s^12p^5$	$1s^22s^12p^4$	6
		$1s^22s^02p^5$	6
Fe XX	$1s2s^22p^4 \rightarrow 1s^22s^22p^3$	$1s^22s^22p^2$	35
		$1s^22s^12p^3$	35
		$1s^22s^02p^4$	35
Fe XX	$1s2s^12p^5 \rightarrow 1s^22s^12p^4$	$1s^22s^12p^3$	47
		$1s^22s^02p^4$	47
Fe XX	$1s2s^02p^6 \rightarrow 1s^22s^02p^5$	$1s^22s^02p^4$	2
Fe XXI	$1s2s^22p^3 \rightarrow 1s^22s^22p^2$	$1s^22s^22p^1$	35
		$1s^22s^12p^2$	35
		$1s^22s^02p^3$	35
Fe XXI	$1s2s^12p^4 \rightarrow 1s^22s^12p^3$	$1s^22s^12p^2$	121
		$1s^22s^02p^3$	121
Fe XXI	$1s2s^02p^5 \rightarrow 1s^22s^02p^4$	$1s^22s^02p^3$	14
Fe XXII	$1s2s^22p^2 \rightarrow 1s^22s^22p^1$	$1s^22s^2$	14
		$1s^22s^12p^1$	14
		$1s^22s^02p^2$	14
Fe XXII	$1s2s^12p^3 \rightarrow 1s^22s^12p^2$	$1s^22s^12p^1$	121
		$1s^22s^02p^2$	121
Fe XXII	$1s2s^02p^4 \rightarrow 1s^22s^02p^3$	$1s^22s^02p^2$	35
Fe XXIII	$1s2s^22p^1 \rightarrow 1s^22s^2$	$1s^22s^1$	2
		$1s^22p^1$	2
Fe XXIII	$1s2s^12p^2 \rightarrow 1s^22s^12p^1$	$1s^22s^1$	47
		$1s^22p^1$	47
Fe XXIII	$1s2s^02p^3 \rightarrow 1s^22s^02p^2$	$1s^22p^1$	35
Fe XXIV	$1s2s^12p^1 \rightarrow 1s^22s^1$	$1s^2$	6
Fe XXIV	$1s2s^02p^2 \rightarrow 1s^22p^1$	$1s^2$	14

betical classification scheme that was first introduced by Gabriel.[7] We should point out that, in our calculations, account has been automatically taken of the LS-term mixing that can occur within each electronic configuration. The LS-term mixing is the result of the diagonalization of the atomic Hamiltonian matrix to form the eigenstates of the total electronic angular momentum J and the parity.

According to Eqs. (2), (8), (10), (16), and (18), together with the discussions presented in Sec. II, the total $K\alpha$ satellite emission spectrum, which is produced by the entire set of fine-structure transitions in Table I, can be represented in the form

$$\epsilon(h\nu)=(h\nu/4\pi)\sum_z\sum_j\sum_k[\alpha_{\rm DR}(z,j\rightarrow k)N_{z+1}N_e + C_{\rm CE}(z,j\rightarrow k)N_zN_e] \times L(z,j\rightarrow k,h\nu)\ , \quad (20)$$

which is a superposition of the contributions associated with the dielectronic recombination and the inner-shell-electron collisional-excitation processes in the various stages of ionization. This representation of the total satellite emission spectrum can be applied to both the low-density region, for which the rate coefficients $\alpha_{\rm DR}(z,j\rightarrow k)$ and $C_{\rm CE}(z,j\rightarrow k)$ are to be evaluated, respectively, by means of Eqs. (7) and (14) and refer to ions initially confined to the ground-state fine-structure levels, and to the intermediate- and high-density regions, where it is permissible to employ the appropriate statistically averaged rate coefficients that are defined, respectively, by Eqs. (11) and (19).

A. Charge-state distributions

The distribution of the iron ions among the various charge states is conventionally expressed in the form

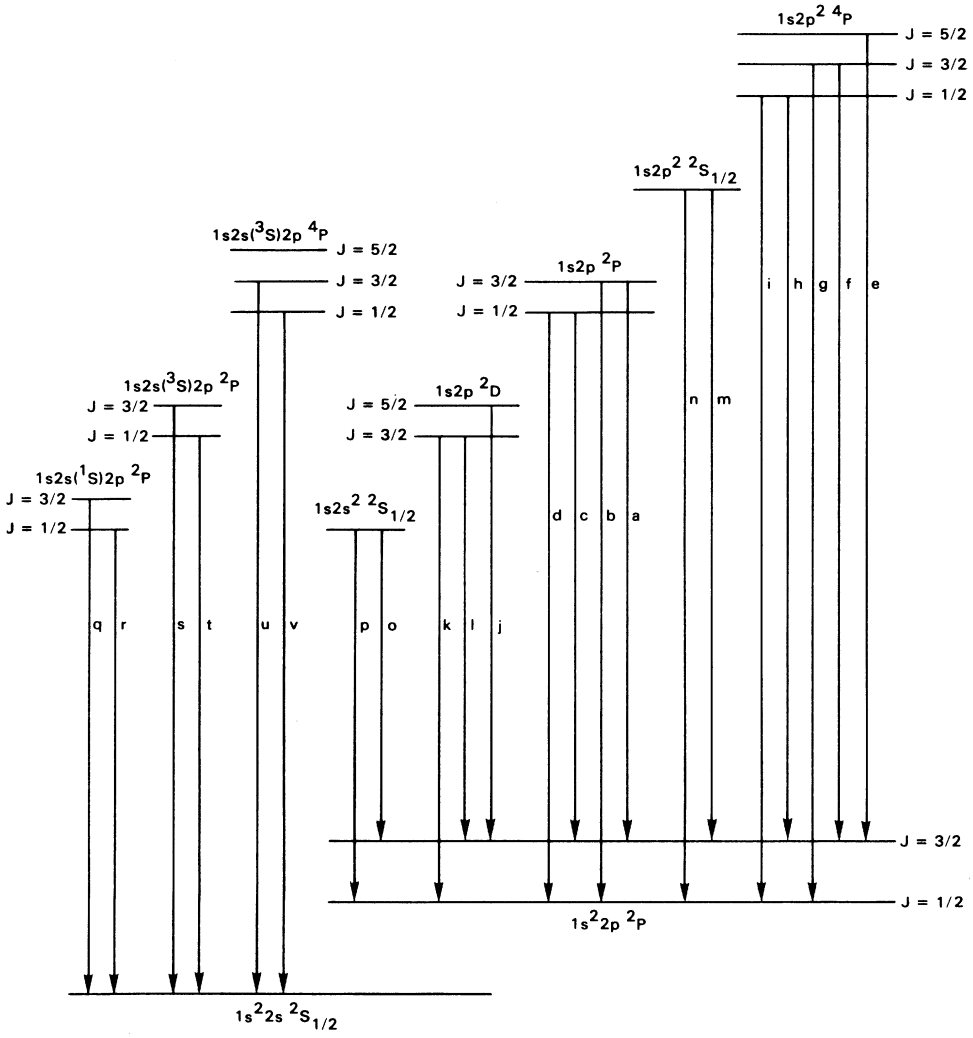

FIG. 1. Spontaneous electric-dipole radiative transitions from autoionizing states belonging the electronic configurations $1s2s^2$, $1s2s2p$, and $1s2p^2$ in the lithiumlike ion Fe XXIV. The alphabetical classification scheme that has been adopted was first introduced by Gabriel (Ref. 7).

$$N_z = (N_z/N_{\mathrm{Fe}})N_{\mathrm{Fe}} , \tag{21}$$

where (N_z/N_{Fe}) are the fractional abundances and N_{Fe} denotes the total number density of the iron ions in all stages of ionization. In this investigation we have employed the corona-equilibrium charge-state distributions (N_z/N_{Fe}) that have been obtained from previously reported calculations,[48] in which electron impact ionization and autoionization following inner-shell-electron collisional excitation from each ground state were assumed to be balanced by spontaneous radiative and dielectronic recombination. The corona-equilibrium charge-state distributions for the ions of interest in the present investigation are illustrated as functions of the electron temperature in Fig. 2, which shows the characteristic property that only a few ionization states have an appreciable abundance within any particular electron-temperature range. The electron-density variation of the charge-state distributions, which becomes important at very high densities, can be properly predicted only by employing a detailed and self-consistent collisional-radiative equilibrium model to explicitly determine the steady-state excited-level populations together with the charge-state distributions.

For astrophysical plasmas which are immersed in intense x-ray radiation fields, Auger electron emission following $1s$ inner-shell-electron photoionization has been demonstrated to be the dominant ionization mechanism.[49] The importance of multiple-electron ionization processes in the presence of intense x-ray radiation fields leads to a very different equilibrium distribution of charge states,[50] in which many ionization stages can have appreciable abundances within certain electron-temperature ranges. In the determination of the total electron-ion recombination rates which enter into the corona-equilibrium ionization-recombination balance calculations, the dielectronic recombination processes that are dominant for the iron ions from Fe XVIII to Fe XXIV within the electron-temperature ranges of their maximum equilibrium abundance have been found to be associated with $2p \rightarrow 2s$, $3p \rightarrow 2s$, $3s \rightarrow 2p$, and $3d \rightarrow 2p$ valence-shell electron radiatively stabilizing transitions. The $2p \rightarrow 1s$ inner-shell-electron radiatively stabilizing transitions, which have been taken into account in the present theoretical prediction of the $K\alpha$ satellite emission spectra, may provide appreciable contributions to the total electron-ion recombination rates only at temperatures that substantially exceed the ionization-recombination equilibrium temperature ranges. These inner-shell contributions to the total dielectronic recombination rates are not expected to be important in the ionization-recombination equilibrium temperature ranges. The $2p \rightarrow 1s$ inner-shell-electron dielectronic recombination processes could play a more important role in a rapidly ionizing nonequilibrium plasma, where the electron temperature can greatly exceed the ionization-recombination equilibrium temperature range. It should be emphasized that the determination of the charge-state distributions, even for equilibrium-plasma conditions, represents a complex calculation, in which systematic account must be taken of a large number of elementary atomic processes.

In plasmas for which ionization-recombination equilibrium is not a valid assumption, it will be necessary to include the contributions representing the various transport processes that can occur in the plasma, such as charged-particle diffusion and thermal conduction, and to determine the charge-state distributions as functions of time from an appropriate set of coupled partial-differential rate equations for the atomic-level populations and for the relevant hydrodynamic variables. The instantaneous values of the electron temperature and density will no longer uniquely characterize the radiative emission spectra in the general nonequilibrium situation, and then it will become necessary to evaluate the $K\alpha$ satellite emission spectra as functions of time.

B. Line-profile functions

In the three separate electron-density regions which are considered in this investigation, the satellite line-

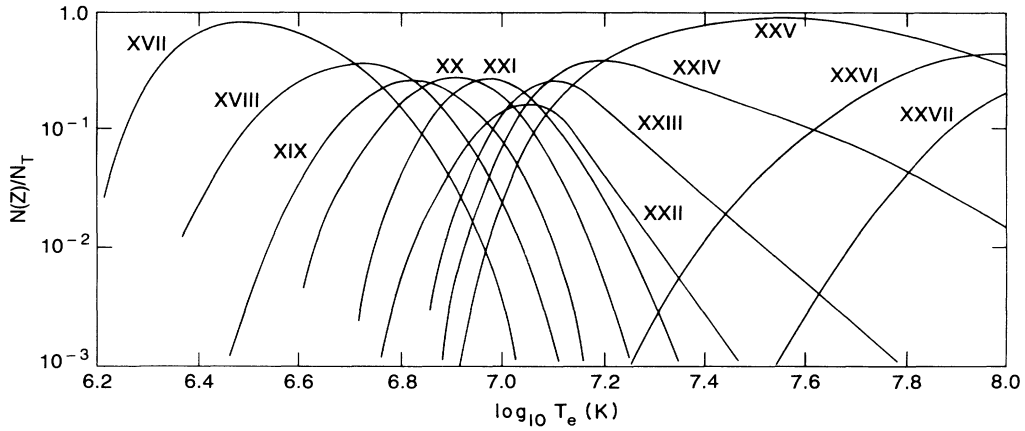

FIG. 2. Coronal ionization-recombination equilibrium charge-state distributions $N(z)/N_T$ (where N_T is the total Fe-ion density N_{Fe}) for the higher ionization states of the iron ions, which have been obtained in previously reported calculations (Ref. 48).

profile functions $L(z,j\rightarrow k,h\nu)$ associated with the isolated-line approximation can be expressed very generally as Voigt line-shape functions. The Voigt line-shape function for each radiation transition $j\rightarrow k$ can be obtained by means of a convolution of a Gaussian line-profile function, which represents the Doppler broadening due to the thermal or turbulent motion of the radiating ions, and a Lorentzian line-profile function, which describes the broadening that is the result of the multitude of elementary atomic autoionization, collision, and radiation processes. We will neglect the density-sensitive Lorentzian broadening of the lower levels k. This is expected to be a good approximation for the $2p\rightarrow 1s$ inner-shell-electron spontaneous radiative transitions. The Voigt parameters $A_{\text{Voigt}}(j\rightarrow k)$, which determine the spectral line shapes, then can be evaluated, in terms of the diagonal elements of the transition rate matrix Q for the upper levels j, by means of the relationship

$$A_{\text{Voigt}}(j\rightarrow k)=Q(j,j)/(4\pi\Delta\nu_D)\ , \tag{22}$$

which provides an indication of the importance of the Lorentzian contribution with respect to the Doppler-broadening component. Since we shall consider only electron densities $N_e\leq 10^{24}$ cm^{-3}, for which one may neglect the density-dependent contributions associated with collisional transitions among the $n=2$ autoionizing levels, the diagonal matrix elements of Q may be evaluated by using Eq. (5). The thermal Doppler-broadening width $\Delta\lambda_D$, measured in angstroms, depends on the Fe-ion temperature T_{Fe}, measured in eV, through the expression

$$\Delta\lambda_D=7.71\times 10^{-5}\lambda(j\rightarrow k)(T_{\text{Fe}}/A_{\text{Fe}})\ , \tag{23}$$

where $\lambda(j\rightarrow k)$ denotes the transition wavelength and A_{Fe} is the atomic weight for iron. In our calculations the Fe-ion temperature T_{Fe} has been taken to be equal to the electron temperature T_e. A two-temperature description would be desirable for application to specific plasma conditions, particularly in the case of short-pulse-duration laser heating. The results of our calculations for the Voigt line-shape parameters, which are presented in Figs. 3 and 4 as functions of the transition wavelength for the two representative temperatures of interest, indicate that the satellite line-profile functions can be represented to a very good approximation, especially at the higher temperature, by the neglect of the spontaneous Lorentzian contributions and the use of the Gaussian Doppler-broadening line-profile functions alone. Only for very high electron densities $N_e\geq 10^{24}$ cm^{-3}, where the $2s\rightarrow 2p$ collisional transition rates connecting the autoionizing levels exceed the autoionization and spontaneous radiative transition rates, would it become necessary to employ the complete Voigt line-shape functions. However, this procedure is not expected to provide an adequate representation at these very high electron densities, because of the breakdown of the isolated-line approximation together with the increasing importance of Stark broadening. It should be emphasized that we have not attempted to incorporate any representation of instrumental broadening, since this is a characteristic of the particular method of spectral observation. In addition, we have ignored the broadening that would be the result of the finite dimensions of the plasma and the spatial and temporal inhomogeneities, because these are detailed plasma properties that cannot be treated within the framework of our general theoretical investigation. The

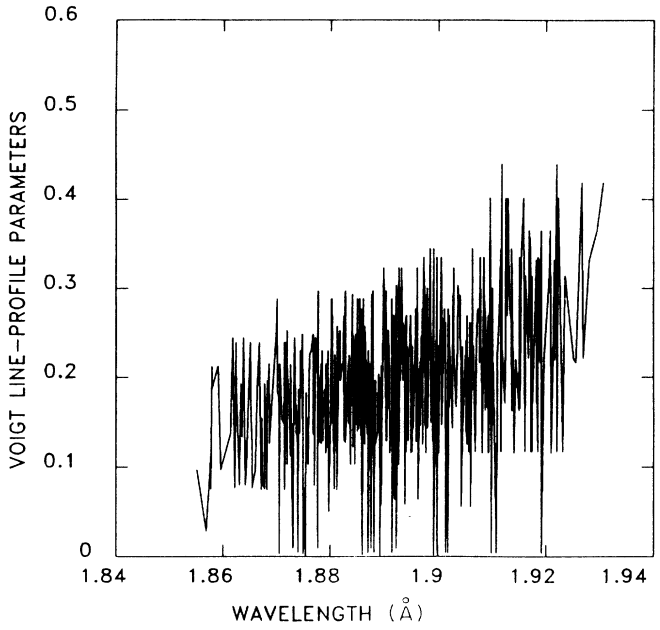

FIG. 3. Voigt line-profile parameters for the $2p\rightarrow 1s$ spontaneous radiative transitions in Table I, evaluated for the electron temperature $T_e=1.0\times 10^7$ K.

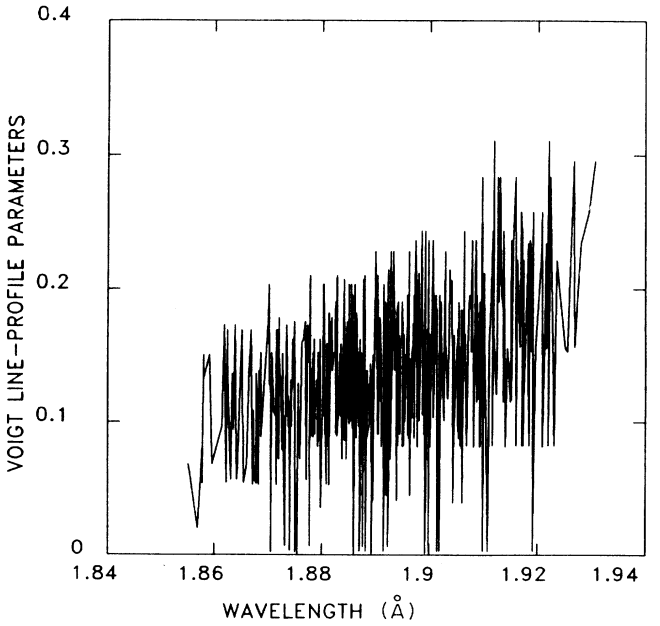

FIG. 4. Voigt line-profile parameters for the $2p\rightarrow 1s$ spontaneous radiative transitions in Table I, evaluated for the electron temperature $T_e=2.0\times 10^7$ K.

satellite line-shape functions employed in our calculations are, accordingly, completely determined by the Fe-ion temperature T_{Fe}, the calculated transition wavelength $\lambda(j \rightarrow k)$, and the required transition wavelength corrections $\Delta\lambda(z)$,[37] which are presented in Table II.

C. Results and discussion

The theoretically predicted $K\alpha$ satellite emission spectra for the iron ions from Fe XVIII to Fe XXIV are presented in Figs. 5–7 for the lower electron temperature $T_e = 1.0 \times 10^7$ K and in Figs. 8–10 for the higher electron temperature $T_e = 2.0 \times 10^7$ K. The spectral intensities that are shown in these figures have been obtained from the evaluation of Eq. (20) without the factor $h\nu/4\pi$ and are, accordingly, expressed in units of photons/sec cm^3. The upper plot in each of these six figures gives the predicted spectrum that is obtained by taking into account only the contributions from the dielectronic recombination processes, while the lower plot presents the complete spectrum that includes the contributions from both the dielectronic recombination and the inner-shell-electron collisional-excitation processes. The emission spectra corresponding to the lower electron temperature reveal the most intense spectral features of the iron ions from Fe XIX through Fe XXIV, while the emission spectra associated with the higher electron temperature are dominated mainly by the prominent satellite lines of the iron ions Fe XXIII and Fe XXIV.

The satellite spectra that have been predicted for solar-flare plasma conditions, which are shown in Figs. 5 and 8, are found to be in very good qualitative agreement with the results of high-resolution x-ray spectral measurements.[1,2,17,18,37] In particular, it is possible to identify the strongest spectral features and to demonstrate good qualitative agreement between the observed and the predicted satellite line intensities. Precise agreement is not expected for a variety of reasons, including the fact that the observed spectra do not exactly correspond to the two representative temperatures that have been selected for our spectral syntheses. The implicit assumption of uniform temperature conditions within the x-ray emitting plasma region is also likely to be a source of discrepancy, but large errors are not expected to result from this assumption. It can be seen that dielectronic recombination provides the dominant mechanism for the excitation of the solar-flare $K\alpha$ satellite spectra. The lithiumlike Fe XXIV satellite line at $\lambda = 1.865\,98$ Å, which is designated by j in the alphabetical classification scheme that was first introduced by Gabriel,[7] is the most well-known spectral feature that is formed almost entirely by dielectronic recombination. Among the strong isolated spectral features that are produced predominantly by inner-shell-electron collisional excitation, the most notable are the lithiumlike Fe XXIV satellite line q at $\lambda = 1.861\,08$ Å and the berylliumlike Fe XXIII transition at $\lambda = 1.870\,51$ Å, which has been customarily designated by β. It should be noted that there are several spectral lines of the heliumlike ion Fe XXV which occur within the photon-wavelength range considered in this investigation. In the alphabetical classification scheme that was first intro-

TABLE II. Wavelength corrections $\Delta\lambda(z)$ which have been added to the calculated wavelengths for the $K\alpha$ satellite transitions in order to obtain the theoretical satellite emission spectra.

Fe ion	$\Delta\lambda(z)$ (Å)
Fe XVIII	0.003
Fe XIX	0.003
Fe XX	0.003
Fe XXI	0.002
Fe XXII	0.002
Fe XXIII	0.0025
Fe XXIV	0.0025

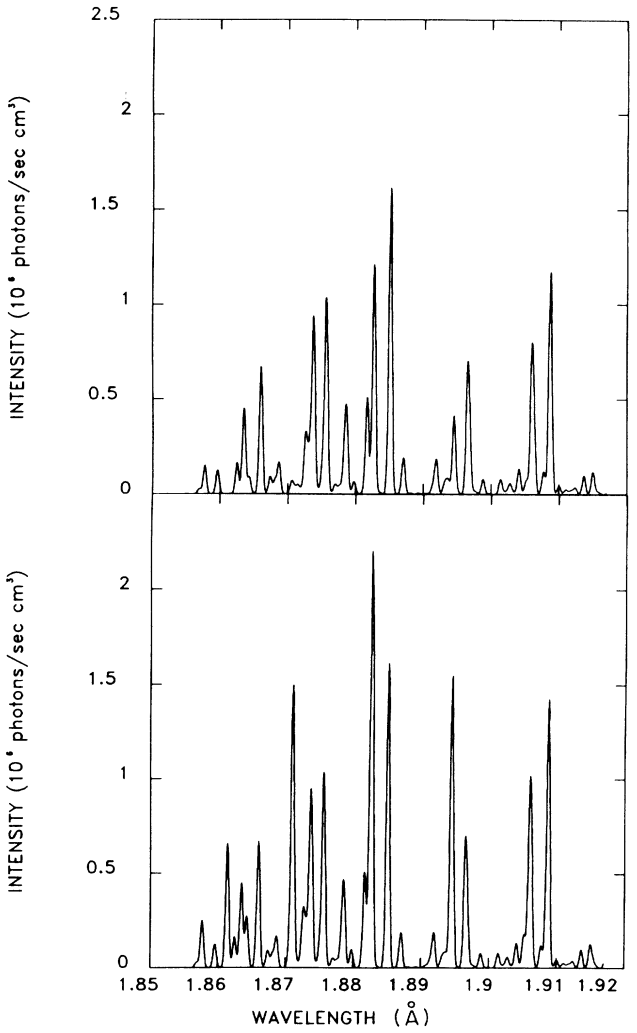

FIG. 5. Predicted $K\alpha$ satellite emission spectra for low-density plasmas ($N_e \leq 10^{12}$ cm^{-3}) corresponding to the electron temperature $T_e = 1.0 \times 10^7$ K, taking into account dielectronic recombination alone (upper spectrum) and dielectronic recombination together with inner-shell-electron collisional excitation (lower spectrum).

duced by Gabriel[7] these Fe XXV lines include the resonance line w at $\lambda = 1.850\,46$ Å, the magnetic-quadrupole transition x at $\lambda = 1.855\,44$ Å, the spin-forbidden line y at $\lambda = 1.859\,61$ Å, and the magnetic-dipole transition z at $\lambda = 1.868\,15$ Å. Since these Fe XXV spectral lines are, strictly speaking, not associated with inner-shell-electron transitions and do not involve autoionizing states, they have not been included in the present set of spectral syntheses. These additional spectral lines should obviously be taken into account in any detailed comparisons with the observed spectra. Doschek and Tanaka[51] have recently reported an investigation of the effect of transient-ionization nonequilibrium conditions on x-ray spectra from solar flares. They have calculated the $K\alpha$ satellite emission spectra assuming time-dependent nonequilibrium charge-state distributions, which differ from the corona ionization-recombination equilibrium distributions employed in the present investigation.

The $K\alpha$ satellite spectra that have been predicted for tokamak-plasma conditions, which are shown in Figs. 6 and 9, are found to be in surprisingly good qualitative agreement with the high-resolution x-ray spectra that have been observed from the Princeton large torus (PLT).[20,52] The PLT $K\alpha$ satellite spectra have been recorded for an electron density $N_e = 5.0 \times 10^{13}$ cm^{-3} and for several values of the central electron temperature in the range $800 \leq T_e \leq 1800$ eV. The most recently recorded PLT $K\alpha$ satellite spectra[52] have a high degree of resolution which is comparable with that of the solar-flare spectra, and the two different observed spectra show re-

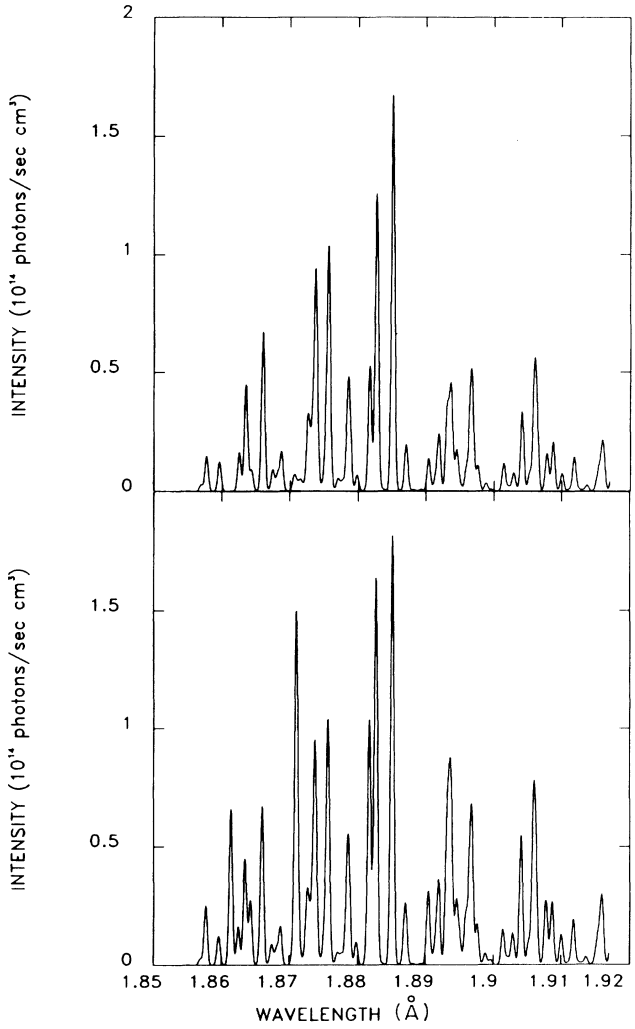

FIG. 6. Predicted $K\alpha$ satellite emission spectra for intermediate-density plasmas ($10^{13} \leq N_e \leq 10^{14}$ cm^{-3}) corresponding to the electron temperature $T_e = 1.0 \times 10^7$ K, taking into account dielectronic recombination alone (upper spectrum) and dielectronic recombination together with inner-shell-electron collisional excitation (lower spectrum).

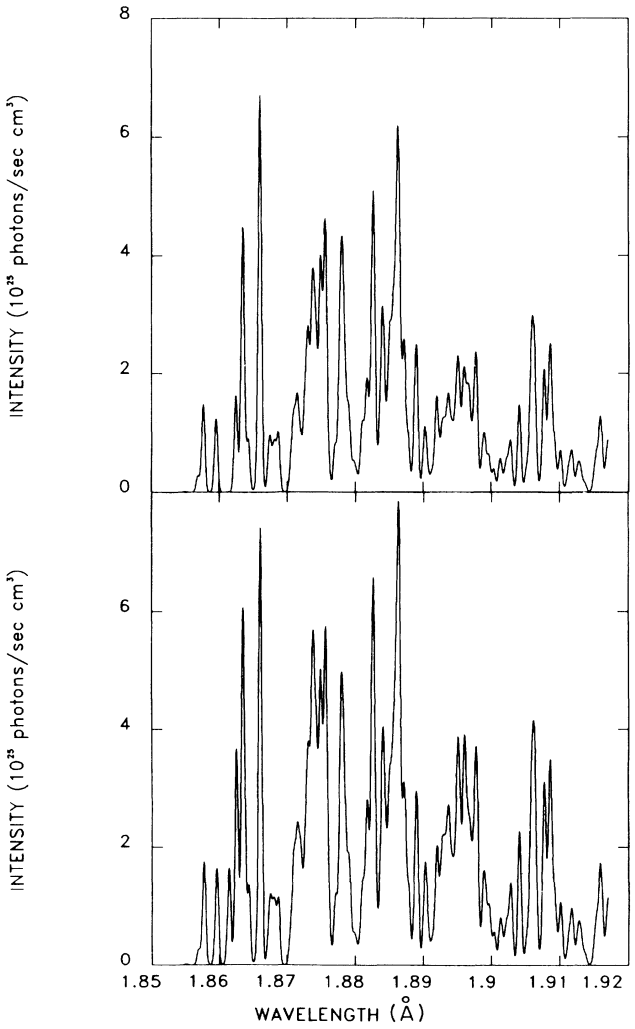

FIG. 7. Predicted $K\alpha$ satellite emission spectra for high-density plasmas ($10^{19} \leq N_e \leq 10^{24}$ cm^{-3}) corresponding to the electron temperature $T_e = 1.0 \times 10^7$ K, taking into account dielectronic recombination alone (upper spectrum) and dielectronic recombination together with inner-shell-electron collisional excitation (lower spectrum).

markable similarities. On the basis of our theoretical model, we would predict a strong electron-density only in the region near the lower electron temperature $T_e = 1.0 \times 10^7$ K $= 862$ eV. This is a consequence of the fact that the ions Fe XIX through Fe XXII, for which the initial-state population variations can occur in the relevant electron-density range, are abundant only in a region near the lower value of the electron temperature. The electron-density dependence is predicted to be less important in the region near the higher value of the electron temperature, where only the Fe XXIII and Fe XXIV spectral lines have significant intensities, and the observed solar flare and tokamak spectra are then expected to be closely similar. The results reported by Phillips, Lemen, Cowan, Doschek, and Leibacher[26] and by Lemen, Phillips, Doschek, and Cowan[27] are based on a rate-equation description of the initial-state population variation, which is clearly more detailed than the statistical distribution employed in the present investigation. However, their initial-state population distributions were not obtained consistently with the ionization-recombination equilibrium charge-state fractions and, accordingly, may not provide a self-consistent representation of the electron-density dependence.

The most probable sources of the small discrepancies that have been found to occur between the predicted $K\alpha$ satellite spectra for tokamak-plasma conditions and the observed PLT spectra are the strong spatial variations in the electron temperature and density. The radial dependence of the electron temperature gives rise to a well-

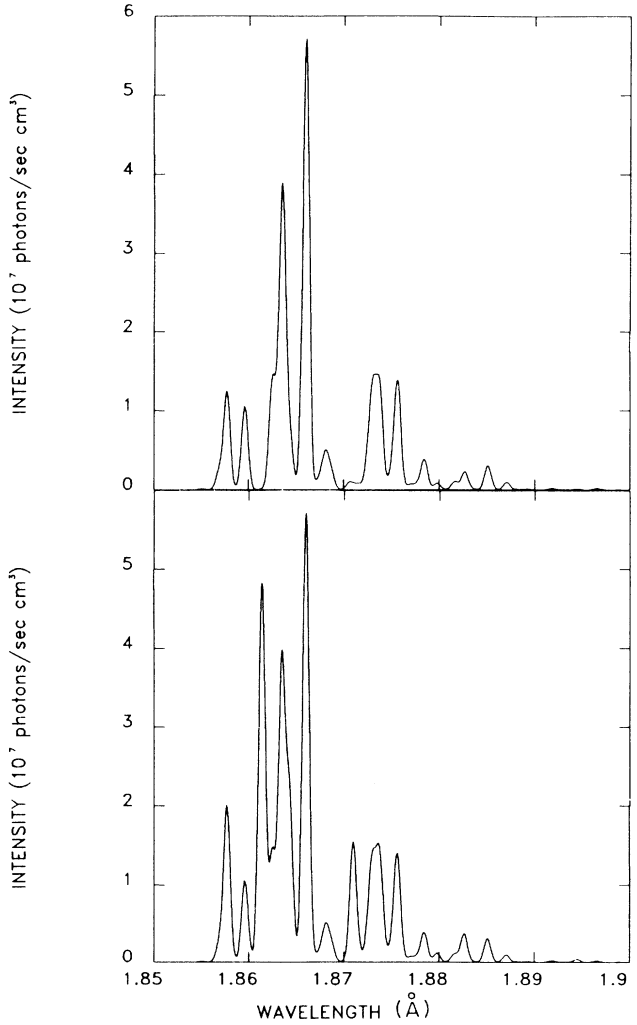

FIG. 8. Predicted $K\alpha$ satellite emission spectra for low-density plasmas ($N_e \leq 10^{12}$ cm^{-3}) corresponding to the electron temperature $T_e = 2.0 \times 10^7$ K, taking into account dielectronic recombination alone (upper spectrum) and dielectronic recombination together with inner-shell-electron collisional excitation (lower spectrum).

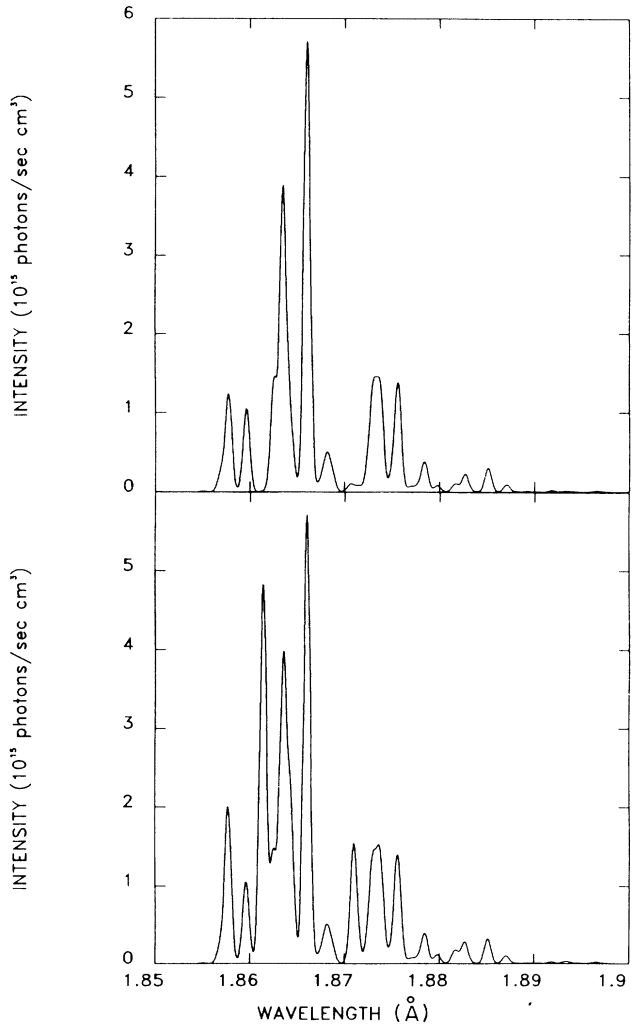

FIG. 9. Predicted $K\alpha$ satellite emission spectra for intermediate-density plasmas ($10^{13} \leq N_e \leq 10^{14}$ cm^{-3}) corresponding to the electron temperature $T_e = 2.0 \times 10^7$ K, taking into account dielectronic recombination alone (upper spectrum) and dielectronic recombination together with inner-shell-electron collisional excitation (lower spectrum).

known shell structure of the various charge-state distributions, in which the more highly ionized ions tend to occur preferentially within the hot central core of the plasma. The departures from the corona ionization-recombination equilibrium distribution, which are the result of radial ion transport processes, are expected to be most severe for the highest charge states, which require relatively long times to attain their equilibrium distributions. Non-Maxwellian electron distributions with substantial high-energy tails and possibly even appreciable anisotropic components are known to occur in tokamak plasmas in which the usual Ohmic heating mechanism is supplemented by an intense microwave absorption process. The extension of the present theoretical model to incorporate a description of nonequilibrium charge-state distributions and non-Maxwellian electron distributions may provide valuable insight into the investigation of ion transport and energy deposition processes in tokamak plasmas.

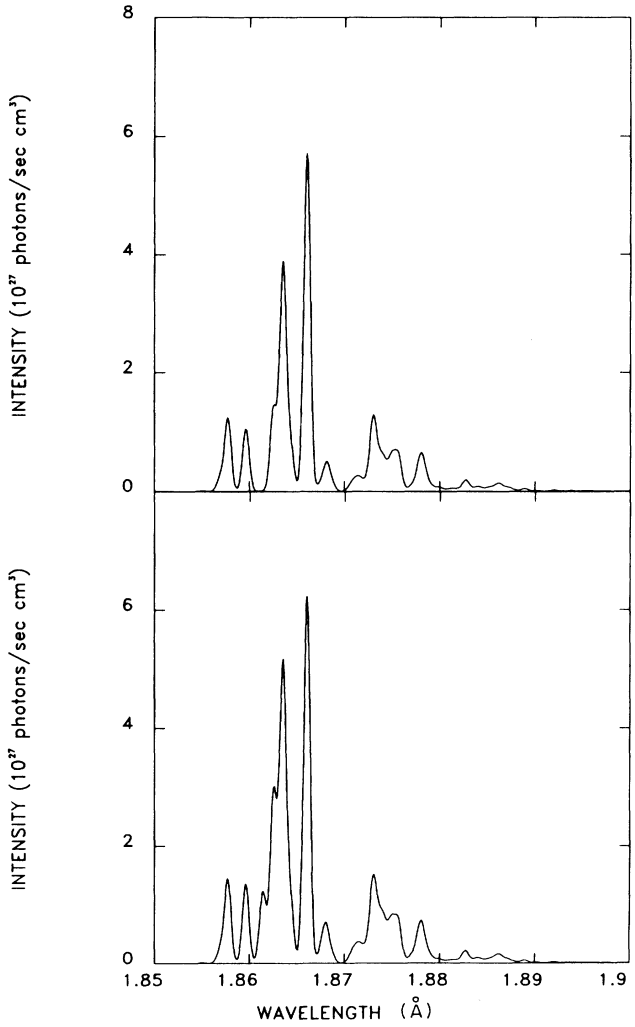

FIG. 10. Predicted $K\alpha$ satellite emission spectra for high-density plasmas ($10^{19} \leq N_e \leq 10^{24}$ cm^{-3}) corresponding to the electron temperature $T_e = 2.0 \times 10^7$ K, taking into account dielectronic recombination alone (upper spectrum) and dielectronic recombination together with inner-shell-electron collisional excitation (lower spectrum).

The synthesized $K\alpha$ satellite emission spectra for laser-produced and vacuum-spark-produced plasma conditions, which are presented in Figs. 7 and 10, are composed of the entire set of transitions given in Table I and, accordingly, represent the major new contribution in the present investigation. High electron densities near $N_e = 10^{20}$ cm^{-3} have also been attained in the plasmas that have been produced by pinches formed in single exploded wires[53] or by implosions formed at the center of symmetrical exploded-wire arrays,[54] and the $K\alpha$ satellite emission spectra that have been observed from these high-density plasmas show about the same degree of resolution as the spectra that have been reported for the laser-produced and vacuum-spark-produced plasmas. Unfortunately, it is not possible to derive any final conclusions from a comparison between the synthesized $K\alpha$ satellite spectra and the x-ray spectra that have been observed from laser-produced,[22] vacuum-spark-produced,[21] and exploded-wire-produced[53,54] plasmas, mainly because of their relatively poor apparent resolution in comparison with the observed solar flare and tokamak spectra. The lower apparent resolution in these high-density spectral observations may not necessarily be a property of the instrumentation used to obtain the data, but may instead be the result of large-scale plasma motions, which could have Doppler broadened the spectral lines substantially beyond what would be predicted on the basis of their thermal widths alone. The predicted $K\alpha$ satellite emission spectra appropriate to the high-electron-density region reveal many additional features with respect to the low- and the intermediate-density results in the case of the lower value of the electron temperature, whereas the differences are much less apparent at the higher value of the electron temperature. The prediction of "richer" spectra at the lower temperature is a direct result of the inclusion of transitions involving the additional bound excited electronic configurations of the initial ions, which not only alters the intensities of the satellite lines that are important at the lower densities but also gives rise to additional lines that occur at new photon wavelengths. The importance of the electron-density sensitivity at the lower value of the electron temperature is clearly the result of the dominance of the $K\alpha$ satellite emission from the ions Fe XIX through Fe XXII, for which the initial-state population variations can occur. Perhaps this electron-density sensitivity of the $K\alpha$ satellite emission spectra will provide a new spectroscopic technique for the study of high-density plasmas, for which there is a particular need for reliable determinations of the electron density and the charge-state distribution.

In Table III,[55] we present a list of the $2p \rightarrow 1s$ inner-shell-electron radiative transitions that provide the dominant contributions in the dielectronic recombination processes. A list of transitions that are dominant in the inner-shell-electron collisional-excitation processes is given in Table IV.[55] These transitions have been specified by giving the initial and final values of the total electronic

angular momenta $J(j)$ and $J(k)$, the calculated photon wavelengths $\lambda(j\rightarrow k)$, the spontaneous electric-dipole emission rates $A_r(j\rightarrow k)$, and the appropriate temperature-independent factor that occurs in the expression for the photon intensity. For dielectronic recombination, the appropriate intensity factor is defined by

$$B_{\mathrm{DR}}(j\rightarrow k)=g_j A_r(j\rightarrow k)Q^{-1}(j,j)\sum_m A_a(j\rightarrow m\varepsilon_{jm}) , \tag{24}$$

and this quantity is routinely evaluated in the relativistic multiconfiguration atomic structure calculations that are carried out using the program of Cowan.[24] Note that the different bound electronic configurations of the initial ions give rise to separate values for this intensity factor, which have been presented in the individually labeled columns in Table III.[55] In the case of inner-shell-electron collisional excitation, the most natural temperature-independent intensity factor is the dimensionless branching ratio for the radiatively stabilizing transition defined by

$$B_r(j\rightarrow k)=A_j(j\rightarrow k)Q^{-1}(j,j) . \tag{25}$$

The $K\alpha$ satellite spectra can be synthesized, for any desired temperature, with good accuracy by employing the reduced data sets given in Tables III and IV.[55]

IV. CONCLUSIONS

In this investigation we have carried out a systematic evaluation of the $K\alpha$ satellite emission spectra for the iron ions from Fe XVIII to Fe XXIV, taking into account all fine-structure components of the $2p\rightarrow 1s$ inner-shell-electron radiative transitions. Predictions for the x-ray emission spectra at two representative values of the electron temperature have been presented for the electron-density regions that are characteristic of solar flares, tokamak devices, and laser-produced and vacuum-spark-produced plasmas. These plasmas have been assumed to have steady-state and optically thin excitation conditions. The predictions that were obtained for solar-flare and tokamak-plasma conditions are found to be in good agreement with previously reported theoretical results, but the present spectra have been obtained using a somewhat different model for inner-shell-electron collisional excitation. The substantially new results that are contained in the present investigation are the synthesized spectra for laser-produced plasmas, which are composed of a large number of additional fine-structure transitions involving bound excited electronic configurations of the initial ions in the dielectronic recombination and the inner-shell electron collisional excitation processes. The inclusion of the additional excited electronic configurations of the initial ions gives rise to an electron-density sensitivity, which may provide a new spectroscopic technique in the study of laser-produced plasmas.

A number of refinements should be incorporated into future extensions of this investigation. Firstly, it would be desirable to carry out a systematic and self-consistent determination of the initial-ion populations together with the charge-state distributions and to incorporate a combined treatment of collisional and Stark broadening for application to the very-high-density region $N_e \geq 10^{24}$ cm^{-3}. The inclusion of precise fully relativistic calculations for the electron-electron correlation and quantum electrodynamical energy corrections for each individual fine-structure component appears to be of particular importance for the exact determination of the location of the various spectral features. More detailed, fully relativistic, distorted-wave calculations for the electron impact excitation rates would also be desirable for a more balanced calculation, in which comparable treatments would be achieved for the dielectronic recombination and inner-shell-electron collisional-excitation processes. Finally, it would also be of interest to systematically include the contributions from autoionizing configurations consisting of $n \geq 3$ electrons, since these contributions could produce detectable alterations in some of the prominent spectral features.

ACKNOWLEDGMENTS

Helpful discussions with M. Bitter, P. Beiersdorfer, and K. W. Hill on the interpretation of the $K\alpha$ satellite emission spectra observed at the Princeton Plasma Physics Laboratory are gratefully acknowledged, and their interest in this theoretical investigation of the $K\alpha$ satellite emission spectra is deeply appreciated. This investigation has been supported by The Office of Fusion Energy, U. S. Department of Energy.

[1]G. A. Doschek, R. W. Kreplin, and U. Feldman, Astrophys. J. Lett. **233**, L157 (1979).
[2]U. Feldman, G. A. Doschek, and R. W. Kreplin, Astrophys. J. **238**, 365 (1980).
[3]M. Bitter, K. W. Hill, N. R. Sauthoff, P. C. Efthimion, E. Meservey, W. Roney, S. von Goeler, R. Horton, M. Goldman, and W. Stodiek, Phys. Rev. Lett. **43**, 129 (1979).
[4]M. Bitter, S. von Goeler, K. W. Hill, R. Horton, D. Johnson, W. Roney, N. Sauthoff, E. Silver, and W. Stodiek, Phys. Rev. Lett. **47**, 921 (1981).
[5]N. J. Peacock, M. G. Hobby, and M. Galanti, J. Phys. B **6**, L298 (1973).
[6]U. Feldman, G. A. Doschek, D. N. Nagel, R. D. Cowan, and R. R. Whitlock, Astrophys. J **192**, 213 (1974).
[7]A. H. Gabriel, Mon. Not. R. Astron. Soc. **160**, 99 (1972).
[8]C. P. Bhalla, A. H. Gabriel, and L. P. Presnyakov, Mon. Not. R. Astron. Soc. **172**, 359 (1975).
[9]F. Bely-Dubau, A. H. Gabriel, and S. Volonte, Mon. Not. R. Astron. Soc. **186**, 405 (1979).
[10]F. Bely-Dubau, A. H. Gabriel, and S. Volonte, Mon. Not. R. Astron. Soc. **189**, 801 (1979).
[11]F. Bely-Dubau, J. Dubau, P. Faucher, and A. H. Gabriel, Mon. Not. R. Astron. Soc. **198**, 239 (1982).
[12]F. Bely-Dubau, P. Faucher, L. Steenman-Clark, J. Dubau, M.

Loulergue, A. H. Gabriel, E. Anotnucci, S. Volonte, and C. G. Rapley, Mon. Not. R. Astron. Soc. **201**, 1155 (1982).
[13]V. L. Jacobs, Astrophys. J. **296**, 121 (1985).
[14]A. Burgess, Astrophys. J. **139**, 776 (1964).
[15]P. L. Hagelstein, M. D. Rosen, and V. L. Jacobs, Phys. Rev. A **34**, 1931 (1986).
[16]M. D. Rosen, J. E. Trebes, B. J. MacGowan, P. L. Hagelstein, R. A. London, D. L. Matthews, D. G. Nilson, T. W. Phillips, D. A. Whelan, G. Charatis, G. E. Busch, C. L. Shepard, and V. L. Jacobs, Phys. Rev. Lett. **59**, 2283 (1987).
[17]K. Tanaka, T. Watanabe, K. Nishi, and K. Akita, Astrophys J. Lett. **254**, L59 (1982).
[18]J. L. Culhane *et al.*, Astrophys. J. Lett. **244**, L141 (1981).
[19]M. Bitter, S. von Goeler, R. Horton, M. Goldman, K. W. Hill, N. R, Sauthoff, and W. Stodiek, Phys. Rev. Lett. **42**, 304 (1979).
[20]K. W. Hill, S. von Goeler, M. Bitter, L. Campbell, R. D. Cowan, B. Fraenkel, A. Greenberger, R. Horton, J. Hovey, W. Roney, N. Sauthoff, and W. Stodiek, Phys. Rev. A **19**, 1770 (1979).
[21]T. N. Lie and R. C. Elton, Phys. Rev. A **3**, 865 (1971).
[22]Yu. A. Mikailov, S. A. Pikuz, G. V. Sklizkov, A. Ya. Faenov, and S. I. Fedotov, Opt. Spektrosk. **42**, 811 (1977) [Opt. Spectrosc. (USSR) **42**, 469 (1977)].
[23]A. L. Merts, R. D. Cowan, and N. H. Magee, Jr., Los Alamos Scientific Laboratory Report No. LA-6220-MS, 1976 (unpublished).
[24]R. D. Cowan, *Theory of Atomic Structure and Spectra* (University of California Press, Berkeley, CA, 1981).
[25]G. A. Doschek, U. Feldman, and R. D. Cowan, Astrophys. J. **245**, 315 (1981).
[26]K. J. H. Phillips, J. R. Lemen, R. D. Cowan, G. A. Doschek, and J. W. Leibacher, Astrophys. J. **265**, 1120 (1983).
[27]J. R. Lemen, K. J. Phillips, G. A. Doschek, and R. D. Cowan, J. Appl. Phys. **60**, 1960 (1986).
[28]R. Mewe, J. Schrijver, and J. Sylwester, Astron. Astrophys. Suppl. **40**, 323 (1980).
[29]R. Mewe and J. Schrijver, Astron. Astrophys. **87**, 261 (1980).
[30]V. L. Jacobs, J. E. Rogerson, M. H. Chen, and R. D. Cowan, Phys. Rev. A **32**, 3382 (1985).
[31]V. L. Jacobs and M. Blaha, Phys. Rev. A **21**, 525 (1980).
[32]L. Armstrong, Jr., C. E. Theodosiou, and M. J. Wall, Phys. Rev. A **18**, 2538 (1978).
[33]S. L. Haan and J. Cooper, Phys. Rev. A **28**, 3349 (1983).
[34]V. L. Jacobs, Phys. Rev. A **31**, 383 (1985).
[35]V. L. Jacobs, J. Cooper, and S. L. Haan, Phys. Rev. A **36**, 1093 (1987).
[36]G. Alber, J. Cooper, and A. R. P. Rau, Phys. Rev. A **30**, 2845 (1984).
[37]J. F. Seely, U. Feldman, and U. I. Safronova, Astrophys. J. **304**, 838 (1986).
[38]P. J. Mohr, Phys. Rev. A **32**, 1949 (1985).
[39]J. Weitsman and P. L. Hagelstein, J. Phys. B **19**, L59 (1986).
[40]H. R. Griem, *Spectral Line Broadening by Plasmas* (Academic, New York, 1974).
[41]V. L. Jacobs and J. Davis, Naval Research Laboratory Memorandum Report No. 4365, 1980 (unpublished).
[42]A. H. Gabriel and K. J. H. Phillips, Mon. Not. R. Astron. Soc. **189**, 319 (1979).
[43]J. F. Seely, U. Feldman, and G. A. Doschek, Astrophys. J. **319**, 541 (1987).
[44]H. A. Bethe, Ann. Phys. (Leipzig) **5**, 325 (1930).
[45]D. Duston, J. E. Rogerson, J. Davies, and M. Blaha, Phys. Rev. A **28**, 2968 (1983).
[46]V. L. Jacobs and B. F. Rozsnyai, Phys. Rev. A **34**, 216 (1986).
[47]D. Duston and J. Davis, Phys. Rev. A **21**, 932 (1980).
[48]V. L. Jacobs, J. Davis, P. C. Kepple, and M. Blaha, Astrophys. J. **211**, 605 (1977).
[49]J. C. Weisheit, Astrophys. J. **190**, 735 (1974).
[50]R. McCray, in *Galactic X-Ray Sources,* edited by P. W. Sanford, P. Laskarides, and J. Salton (Wiley, New York, 1982).
[51]G. A. Doschek and K. Tanaka, Astrophys. J. **323**, 799 (1987).
[52]M. Bitter, P. Beiersdorfer, and K. W. Hill (private communication).
[53]P. G. Burkhalter, C. M. Dozier, C. Stallings, and R. D. Cowan, J. Appl. Phys. **49**, 1092 (1978).
[54]P. Burkhalter, J. Davis, J. Rauch, W. Clark, G. Dahlbacka, and R. Schneider, J. Appl. Phys. **50**, 705 (1979).
[55]See AIP document No. PAPS PLRAAN-39-2411-12 for 12 pages of Tables III and IV. Order by PAPS number and Journal reference from American Institute of Physics, Physics Auxiliary Publication Service, 335 East 45th Street, New York, New York 10017. The prepaid price is $1.50 for each microfiche (98 pages) or $5.00 for photocopies of up to 30 pages. Airmail additional Make checks payable to the American Institute of Physics.